Received: 3 December 2021 | Revised: 23 January 2022 | Accepted: 8 February 2022

DOI: 10.1002/jor.25297

RESEARCH ARTICLE

Journal of Orthopaedic Research®

Sex-based differences in the severity of radiation-induced arthrofibrosis

Samuel N. Rodman[1,2] | Paige N. Kluz[1,2,3] | Madeline R. Hines[1,2] | Rebecca E. Oberley-Deegan[4] | Mitchell C. Coleman[1,2]

[1]Department of Radiation Oncology, Free Radical and Radiation Biology Program, Holden Comprehensive Cancer Center, University of Iowa, Iowa City, Iowa, USA

[2]Department of Orthopedics and Rehabilitation, University of Iowa Hospitals and Clinics, Iowa City, Iowa, USA

[3]Department of Pathology and Laboratory Medicine, Human Leukocyte Antigens (HLA) Laboratory, University of Wisconsin-Madison, Madison, Wisconsin, USA

[4]Department of Biochemistry and Molecular Biology, University of Nebraska Medical Center, Omaha, Nebraska, USA

Correspondence
Mitchell C. Coleman, Department of Radiation Oncology, Free Radical and Radiation Biology Program, Holden Comprehensive Cancer Center, University of Iowa, Iowa City, IA 52242, USA.
Email: mitchell-coleman@uiowa.edu

Funding information
National Institute of Arthritis and Musculoskeletal and Skin Diseases, Grant/Award Number: AR070914

Abstract

As cancer survivorship increases, so does the number of patients that suffer from the late effects of radiation therapy. This includes arthrofibrosis, the development of stiff joints near the field of radiation. Previous reports have concentrated on skin fibrosis around the joint but largely ignored the deeper tissues of the joint. We hypothesized that fat, muscle, and the joint tissues themselves would play a more significant role in joint contracture after radiation than the skin surrounding the joint. To address this hypothesis, we irradiated the right hind flanks of mice with fractionated and unfractionated dose schedules, then monitored the mice for 3 months postradiotherapy. Mice were euthanized and physiological indications of arthrofibrosis including limb contracture and joint resting position were assessed. Stifle (knee) joints demonstrated significant arthrofibrosis, but none was observed in the hock (ankle) joints. During these studies, we were surprised to find that male and female mice showed a significantly different response to radiation injury. Female mice developed more injuries, had significantly worse contracture, and showed a greater difference in the expression of all markers studied. These results suggest that women undergoing radiation therapy might be at significantly greater risk for developing arthrofibrosis and may require specific adjustments to their care.

KEYWORDS
cancer/tumors, pathophysiology, trauma

1 | INTRODUCTION

The American Cancer Society estimates that in 2019 there were 16.9 million cancer survivors in the United States, and within the next decade that number will grow to over 20 million.[1] Roughly 29% of cancer survivors have been treated with radiation, and about 50% of all cancer patients will receive radiation treatment.[2–4] With rising survivorship, there will be a large population suffering from late effects of radiation therapy that accompany cancer treatment, making normal tissue toxicity a growing concern in the medical community.[5] Joint contracture and arthrofibrosis (articular joint fibrosis) are two examples of disease resulting from normal tissue injury that affect the quality of life of cancer survivors.

Normal tissue fibrosis can occur in a variety of locations depending on the type of cancer and the treatment choices made by the presiding physician in designing the radiation field. For patients who

receive radiation near or within an articular joint space, joint contracture is a prescient concern. Those most often affected include breast cancer survivors,[6] head and neck cancer survivors,[7] and sarcoma survivors.[8] In cases of radiation-induced arthrofibrosis, patients typically begin to develop pain and immobility in the affected joint then eventually lose range of motion, potentially progressing to full paralysis of the affected joint. A major problem in the treatment of fibrotic lesions is that the primary treatment consists of surgical resection and/or forced mobilization of fibrotic tissue, which provides only temporary relief and can result in the development of more extensive arthrofibrosis.[9,10]

Sex differences in arthrofibrosis after traumatic injuries such as anterior cruciate ligament (ACL) tears have been studied, with development of fibrosis has been reported to be 2.5%–2.8% more likely in females compared to males.[11–13] This difference has been attributed to differences in immunological response, with women demonstrating a higher innate and adaptive immune response leading to increases in inflammation and inflammatory signaling.[14] In terms of radiation exposure to nonorthopedic tissues, women have also been shown to be more radiosensitive long term than men at equal doses of ionizing radiation.[15] With the rising number of radiation-treated cancer survivors experiencing effects from radiation therapy, a better understanding of arthrofibrosis and any sexual dimorphism is needed to develop effective interventions.

Here we describe a murine model with which to study interactions between various tissues of the articular joint during radiation-induced arthrofibrosis and examine prototypic therapies for prevention. For this report, we hypothesized that indications of arthrofibrosis after radiotherapy would not be confined to the skin and that the deeper tissues of the joint would be involved in any observed joint contracture. Of particular interest to fibrosis development, adipose tissue deposition is critical to fibrosis development in lung and other tissues, with macrophage-derived transforming growth factor beta signaling causing preadipocyte-to-myofibroblast transformation.[16] Radiation exposures cause preadipocytes to lose proliferative and differentiation capacity indicated by the loss of transmembrane marker CD34.[17] Adipose tissue adjacent to joint space in the radiation field seems likely to contribute to fibrotic development.

As a prototypic application of the model, we hypothesized that administration of superoxide dismutase (SOD) mimetics utilized in other tissues could alter fibrosis through modulation of the local redox environment during radiation exposures. SOD mimics such as those used in this study (GC4403 and BMX-001) have been used recently as radioprotective agents in normal tissue that do not confer protection to tumors and may also increase radiation toxicity in cancer cells.[18] This made these compounds attractive as potential acute protective treatments in this model development experiment especially since GC4403 is only known to react with superoxide while BMX-001 is known to react with superoxide and hydrogen peroxide[19]; however, here we report no clear treatment effect. We note that the effectiveness of drug delivery to the tissues of the joint was impossible to assess and mimetics were only applied acutely, in contrast to more recently published approaches using different dosing schedules.[20,21] Mice were irradiated using two prototypic, clinically relevant dose schedules including fractionated doses of 5 Gy and a bolus dose of 25 Gy. Following the described doses of IR and a 12-week observation period, mice were assessed for physiological indications of arthrofibrosis including limb contracture and stifle and hock resting position. As stated, we observed no difference with SOD mimetic treatment; however, when we pooled the ineffective treatments and sham-treated mice into their respective radiation dose groups a strongly significant difference between male and female arthrofibrosis after radiation injury was observed. Stifle joints were then processed for immunohistochemical analysis of markers of fibrosis, where we observed significant increases in α-smooth muscle actin (α-SMA) and NOX4, as well as a decrease in adipose CD34 in fibrotic joints that were more significant in females than males. This observation supports the hypothesis that tissues deeper than skin are involved in joint contracture and indicates that female patients may be at greater risk of arthrofibrosis due to radiotherapy.

2 | MATERIALS AND METHODS

2.1 | Mouse arthrofibrosis model

Animals were housed in the animal care facility at the University of Iowa, which has a PHS Animal Welfare Assurance, is registered with the US Department of Agriculture and is accredited by the Association for Accreditation of Laboratory Animal Care. All animal protocols were reviewed by the Institutional Animal Care and Use Committee. 62 mice (C57B6J; 35 females and 27 males) 8–12 weeks old were utilized for this study and no mice were censored from the study. 27 mice (10 male; 17 female) received one 25 Gy dose of irradiation and 35 mice (17 male; 18 female) received five doses of 5 Gy over a course of 5 days. The typical dose constraint for the most biologically relevant human analog, the femoral head, is 50 Gy.[22] To stay under that constraint, we chose five fractions of 5 Gy with an EQD2 of 40 Gy, and the single dose of 25 Gy was intended as a positive control for the development of fibrosis. Mice were anesthetized through an intraperitoneal injection of ketamine/xylazine, and then the right hind limb was irradiated using a Pantak Therapax DXT 300 X-ray machine (200 kVp with added filtration of 0.35 mm copper and 1.5 mm aluminum). Following irradiation, mice were monitored for signs of radiation damage and were killed 12 weeks later. A small number of mice developed severe enough skin lesions at sites of radiation therapy that topical ointment was applied.

2.2 | Drug handling and in vivo treatment

SOD mimics were given five times to the fractionated group and once to the bolus dose group immediately before radiation exposures. GC4403 was provided by Galera Therapeutics. GC4403 was dissolved in saline buffered with bicarbonate at a molarity of 8.3 mM,

sterile filtered, and delivered intraperitoneally at 9 mg/kg between 45 and 60 min before irradiation. BMX-001 was provided as a generous gift by Dr. Rebecca Oberley-Deegan. BMX-001 was dissolved in bicarbonate buffered saline at a molarity of 354.6 μM, sterile filtered, and delivered intraperitoneally at 1 mg/kg between 45 and 60 min before irradiation. Control mice received an equivalent volume of saline at the same time.

2.3 | Physiological indications of injury and fibrosis

Within one hour of sacrifice, mice were photographed from both the irradiated and nonirradiated side. Using a goniometer, legs were pulled taut by the toes, released to return to a natural resting position, and the resting angle of both the stifle and hock were measured on either side of each mouse. A decrease in resting angle on the irradiated side compared to the contralateral is indicative of limb contracture and the presence of fibrosis in or around the joint. Leg length was measured by pulling the leg taut by hand without tearing any potential fibrotic lesions and measuring from the ball of the hip to the end of the toes. When a difference between left and right legs was detected, measurements were retaken to ensure accurate and consistent results. While the growth plate could be damaged and result in shorter irradiated legs than nonirradiated, in this short time leg shortening is most likely indicative of a reduced extension ability and thus leg contracture and fibrosis. For heavily scarred or contracted mice, once measurements had been taken, we removed the skin, and the legs were remeasured to ensure accurate leg length and stifle angle measurements. Skin removal did not alter the resting angle or leg length results in any of the mice assessed. Following all measurements, the hind limbs were removed and divided into stifle and hock samples that were fixed in 10% neutral buffered formalin (NBF) for 3 weeks.

To determine the degree of injury after irradiation, study animals were assessed daily for the duration of the study. Any apparent irregularity including fur loss, fur color change, dermatitis, contracture, erythema, or limb swelling was noted. All injuries were considered an equivalent indication of injury for the purposes of the charts shown here.

2.4 | Histological preparation

Following fixation, tissues were processed for histological endpoints. Bone samples were first decalcified in 10% formic acid for two days followed by three days in 5% formic acid. All samples were then dehydrated in stepwise increases in EtOH, cleared in xylene, and soaked in liquid paraffin. Samples were embedded in paraffin wax with the stifles positioned to produce coronal sections of the stifle. Sectioning was performed on a microtome to produce 5 μm sections on glass slides. Slides were deparaffinized and either stained with hematoxylin and eosin (H&E) or prepared for immunohistochemistry. Sections were digitized using a stage scanner microscope (Olympus VS110, Olympus America Inc.) at a resolution of 322.25 nm/pixel.

2.5 | Capsular thickness measurements

Images were taken from scans of hematoxylin and eosin-stained sections. These coronal sections were examined for regions with intact and clearly defined articular capsule and synovial membrane surrounding the joint. Areas, where the capsule had minimal artifactual disruption, were identified for measures of the width of the capsular tissue. This increased thickness is associated with synovitis, inflammation, and fibrosis in a wide variety of orthopedic settings. Three regions of interest were examined at 10X magnification in ImageJ and eight manual measurements of capsular thickness were taken per region.

2.6 | Immunohistochemistry

Slides were prepped via antigen retrieval by exposure to 10% citric acid at 65°C for 24 h. A solution of 3% hydrogen peroxide was added to quench any peroxidase activity, and samples were put in blocking solution (10% normal serum, 1% bovine serum albumin [BSA], 0.1% Tween in phosphate-buffered saline [PBS]) for 40 min. Primary antibodies-anti-α-SMA (Abcam ab124964), anti-NOX4 (Millipore ABC271), or anti-CD34 (Abcam ab81289) were diluted in blocking solution (10% normal goat serum, 1% BSA, 0,1% Tween in PBS) and samples were incubated for 1 h at room temp, then overnight at 4°C. Following three rinses with PBS, secondary antibody biotinylated goat anti-rabbit IgG (Vector BA-1000) was added and incubated for 30 min. Kits from Vector laboratories (ABC PK-8200 and DAB SK-4100) were used to develop the slides and, following counterstain with hematoxylin, slides were fixed with Permount (Fisher Chemical SP15-500), coverslips were applied, and slides were dried. Slides were digitized using the Olympus VS110 stage scanning microscope with a 40X objective. Once slides were scanned, samples were scored according to either intensity of staining (0–5) or degree of colocalization between two targets across serial sections (0–-3). A guide for the intensity of staining was generated for each batch of immunohistochemistry that was done where a score for intensity of 0 would indicate little to no staining while a score of 5 would indicate highly saturated stain. A similar guide was generated for colocalization scoring where a score of 0 indicates that on serial (i.e., sequential) slides α-SMA and NOX4 positive staining did not overlap, while a score of 3 indicates that the two stains were positive at the same locations on the contiguous sections. Four areas of interest were taken for each slide scanned and scored by three blind scorers.

2.7 | Statistical analysis

All data shown include at least three male and three female mice. Statistical analysis was performed with Student's *t* test to compare individual groups, and with one- or two-way analysis of variance ANOVA with Fisher's LSD for multiple comparisons and Mantel–Cox

log-rank tests were used to for survival curves. Scored section averages were compared using the nonparametric Friedman test or with the Kruskal–Wallis test. All analysis was done using GraphPad Prism 9.1.0.

3 | RESULTS

Mice were treated with one dose of 25 Gy or five doses of 5 Gy and allowed to heal for 12 weeks after irradiation. During this time the mice were closely monitored with minimal indications of discomfort observed until the appearance of radiation burns at around 3 weeks in roughly 30% of mice. No significant weight loss was noted from the first day of irradiation to the day of euthanasia, despite several mice developing severe radiation burns and hind limb joint contracture. Once the mice were killed, the leg length of each mouse was measured on both the irradiated side and the contralateral side. The length of the irradiated leg was subtracted from the contralateral leg of each mouse to assess leg shortening. When comparing the SOD mimic treated mice with the control group, we saw no significant difference in any of the endpoints measured as shown in Figure S1. Functional data from the ineffective SOD mimic treatments and the sham-treated mice were then pooled to provide stronger statistical support for the physiological characterization of arthrofibrosis after radiation exposure. Figure 1A shows that in both dose schedules irradiated legs were significantly shorter than the contralateral legs. Both IR doses were significant compared to the null (difference of 0 cm) in the whole cohort.

In addition to the leg shortening measurements, hock and stifle joint angle measurements of both legs of each mouse were taken to estimate the degree of joint contracture. Figure 1B,C shows angle measurements of the irradiated versus the unirradiated legs. The fractionated group showed no difference in angle measure when comparing the irradiated and unirradiated legs, and the hock joint showed no difference in the single-dose treatment group (Figure 1B). However, the stifle joint did show significant contracture in the

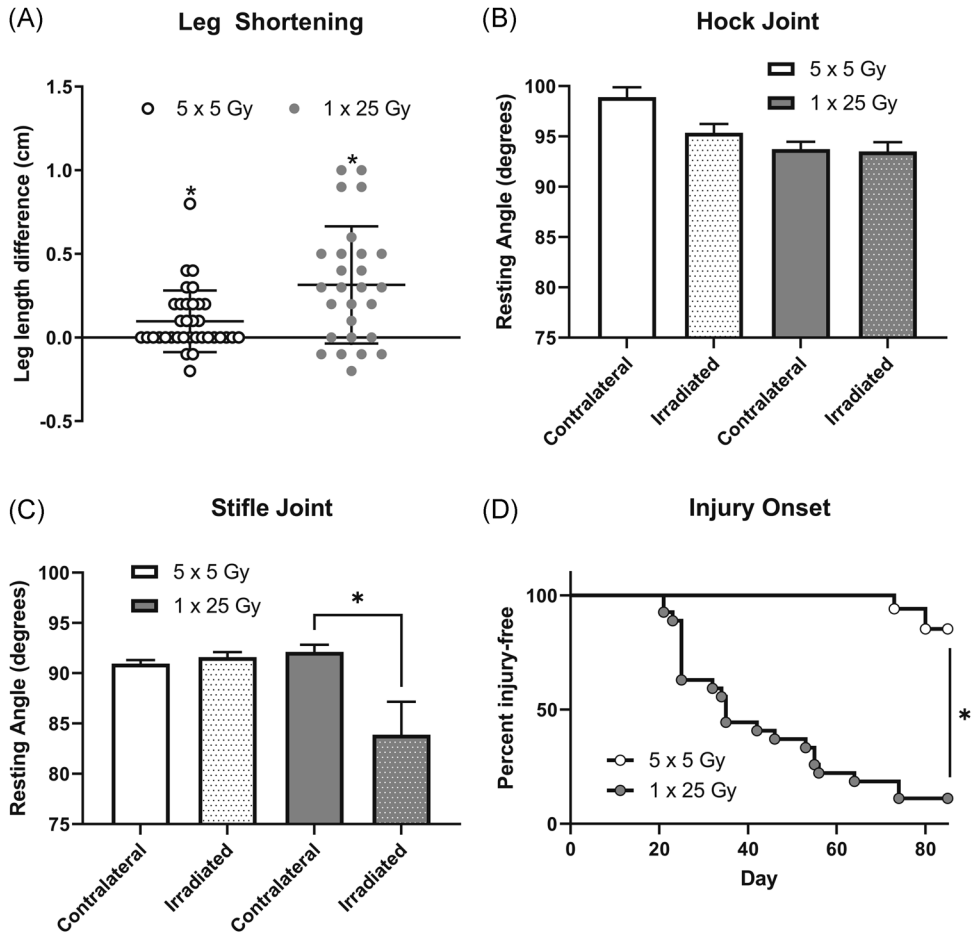

FIGURE 1 Irradiated legs were significantly shorter than the contralateral leg in both the fractionated and single-dose groups. The length of the irradiated leg was subtracted from the length of the contralateral to determine how much shortening had occurred (A). $n = 35$ (5 × 5 Gy), $n = 27$ (1 × 25 Gy). $^*p < 0.05$, t test column statistics of mean compared to theoretical mean of 0. Resting angles were measured post-sacrifice and graphed by radiation dose in the hock (B) or stifle joints (C). Dotted bars indicate irradiated legs, clear bars indicate contralateral legs. $n = 35$ (5 × 5), $n = 27$ (1 × 25) $^*p < 0.05$, paired t test. Percent injury-free survival is shown between the single and fractionated groups (D). $n = 35$ (5 × 5), $n = 27$ (1 × 25) $^*p < 0.0001$ log-rank (Mantel–Cox)

single-dose group (Figure 1C). Mice were monitored daily following radiation for the duration of 12 weeks, and injuries including fur loss, fur color change, dermatitis, and obvious contracture were noted. Surprisingly some mice never developed any visible injury, so we combined all visual injury and plotted a survival curve where the initiation of injury was counted as a loss. As expected from the fractionation, when comparing the dose schedules in terms of the appearance of injury from radiation, the single-dose mice began developing visible injuries at Day 21, while the fractionated dose group did not show injuries until Day 73 (Figure 1D). All visible injuries including alopecia or vitiligo and dermatitis, were combined and the curves were significantly different.

Stifle joints were analyzed for tissue-level, molecular indications of disease. We first examined global (male and female combined) differences in capsular thickness, uniformity of adipose tissue in the joint, and morphological changes between the different treatment groups. Figure 2 shows the difference between fibrotic and healthy capsule and synovium following radiation. Even in tissues that did not show outward signs of contraction, the irradiated tissue shows positive staining for α-SMA, a sign of myofibroblast presence. The capsule in the unirradiated leg is smooth, only a few cells thick, and the nuclei are flat and long, while the irradiated leg shows irregular thickness, broader nuclei, and a lack of cohesion in the capsule tissue. Quantitation of this difference shown in Figure 2C demonstrated a trend towards increased thickness in the irradiated leg compared to the unirradiated leg. It also appears that the single dose of radiation experienced more thickening than the fractionated doses.

There was a significant difference in manifestation of injury between the pooled male and female mice during recovery. Figure 3 shows the percent of mice that were injury-free following the radiation treatment separated by sex. After noting the global incidence of disease but the more severe incidence of injury among females, the resting angle and leg length measurements were separated by male and female and normalized to each mouse's internal contralateral control as shown in Figure 4. The resting angle was significantly lower in the females compared to the males of the single dose of 25 Gy mice, and the females experienced a significant reduction when comparing the fractionated and bolus groups (Figure 4A). The leg length loss was also significantly worse for females compared with males in the bolus dose group as well as between the females of the fractionated and bolus groups (Figure 4B).

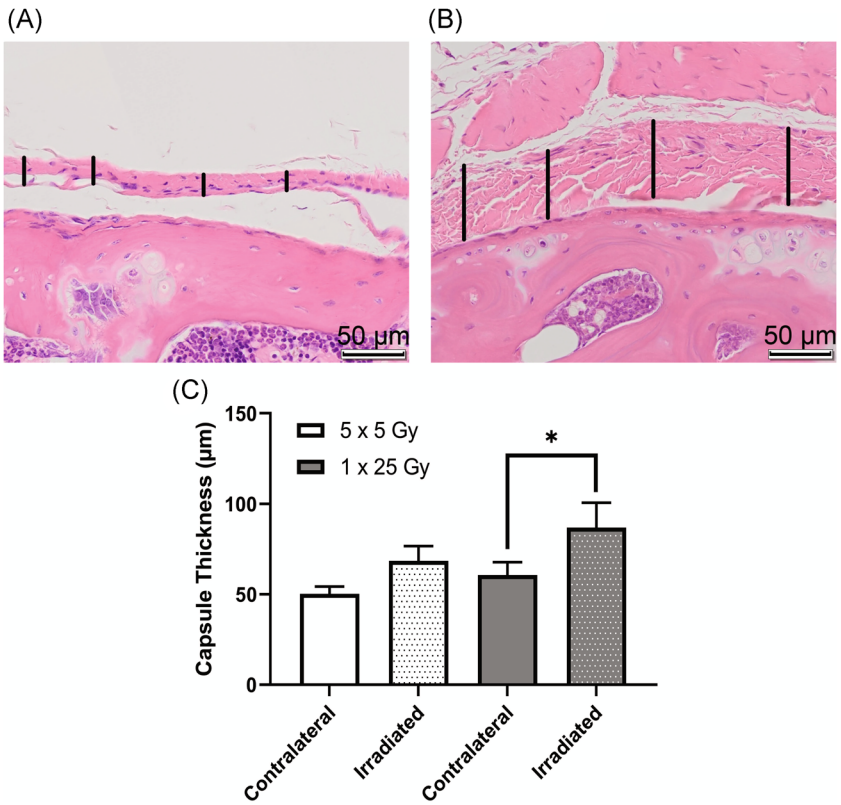

FIGURE 2 Irradiated capsule was significantly thicker in the mice that received a single dose of 25 Gy. Hematoxylin and eosin (H&E)-stained slides of coronal sections show healthy joint capsule from the contralateral leg of a mouse that received fractionated doses of radiation (A) and inflamed capsule tissue from the irradiated leg of a mouse that received a single bolus dose of radiation (B). Capsular thickness is indicated by vertical black bars, scale bar is 50 µm. Representative images were taken from the proximal edge of the femur (lower half of image) with the capsular and synovial tissue in the center of the image. Images were analyzed using ImageJ length measurement tool to determine average capsule thickness in µm (C). Dotted bars indicate irradiated legs, clear bars indicate contralateral legs. 5 × 5 Gy (n = 8); 1 × 25 Gy (n = 5); *p < 0.05, two-way analysis of variance (ANOVA)

To examine molecular indications of the extent of radiation-induced arthrofibrosis in the study, immunohistochemical analyses were performed for αSMA, NOX4, and CD34 on serial, coronal sections of intact stifle joints. Once slides were stained and scanned, they were scored by three independent scorers. In Figure 5 the average of the semi-quantitative scores for αSMA is shown for the fractionated and single-dose groups as well as the histogram plots for the frequency of each score (Figure 5C,D). While there were no significant differences between the two groups of mice analyzed as a whole (Figure 5A), when the groups are stratified by sex the females of the single bolus dose group show a significant increase compared to both the males of the single-dose group as well as the females of the fractionated doses (Figure 5B). Example images of negative staining in the fat pad are shown in Figure 5E and positive staining are shown in Figure 5F. Similarly, in the NOX4 stained slides, shown in Figure 6, the overall comparison shows a trend towards increase NOX4 staining in the single dose of 25 Gy compared with the five doses of 5 Gy (Figure 6A). When the scores are stratified by sex, females stain significantly more than the males in the single bolus dose group (Figure 6B). The histogram plots for both the dose schedule groups are also shown (Figure 6C,D) and example images of negative (Figure 6E) and positive (Figure 6F) staining are shown. NOX4 and αSMA scoring of serial sections revealed colocalization of these indicators within the tissue, Figure S2. Interestingly, changes in capsular thickness did not show a sex-dependent difference, Figure S3.

To further describe connections between this fibrosis and adipocyte biology, preadipocytes in the stifle infrapatellar fat pad were stained using anti-CD34 and scored, shown in Figure 7 and example. There is a significant decrease in CD34 staining in the single-dose group when comparing the irradiated and contralateral average scores (Figure 7A), indicating depletion of pre-adipocyte populations. When the scores are stratified by sex, the females are significantly higher scorers than the males in the single dose of 25 Gy group (Figure 7B) indicating a higher baseline population of pre-adipocytes, however, the overall decrease in CD34 staining between contralateral and irradiated legs is driven by females in the single-dose group indicating greater sensitivity in female pre-adipocytes. Histogram plots show the distribution of scores in the fractionated (Figure 7C) and the single-dose (Figure 7D) groups, also shown are representative images of both negative (Figure 7E) and positive (Figure 7F) staining.

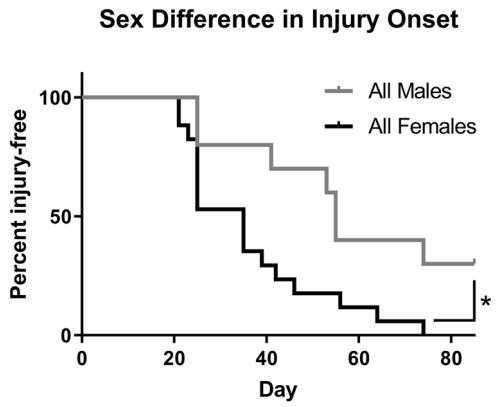

FIGURE 3 Female mice developed injuries more often and more quickly than male mice. Injuries of the mice that received a single dose of 25 Gy were binned so that any visible difference including alopecia, vitiligo, dermatitis, and contracture were counted as a loss. Males ($n = 10$); Females ($n = 17$); $^*p < 0.05$, log-rank (Mantel–Cox) test

4 | DISCUSSION

Previous laboratory work done on radiation-induced arthrofibrosis utilized large single doses of radiation delivered to the hind limb of C_3Hf/Bu mice and a recovery period of hundreds of days.[23] The authors argued that skin contraction is largely responsible for leg

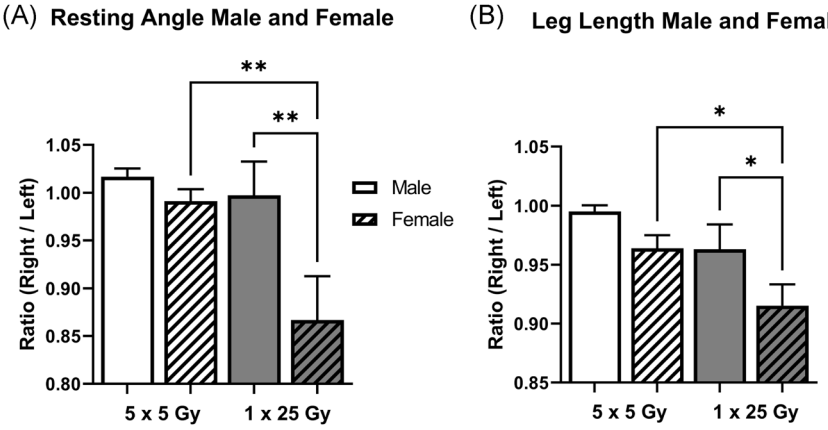

FIGURE 4 Female mice contributed the most to the differences in resting angle and leg length. Previously shown data from Figure 1 is separated by radiation dose and sex for the resting angle (A) and leg length (B) and measurements are normalized to the contralateral. White bars indicate 5 × 5 Gy mice, while gray bars indicate 1 × 25 Gy mice. Clear bars indicate male and dashed bars indicate female. 5 × 5 Male ($n = 17$); 5 × 5 Female ($n = 18$); 1 × 25 Male ($n = 10$); 1 × 25 Female ($n = 17$); $^{**}p < 0.007$, one-way analysis of variance (ANOVA); $^*p < 0.05$, one-way ANOVA.

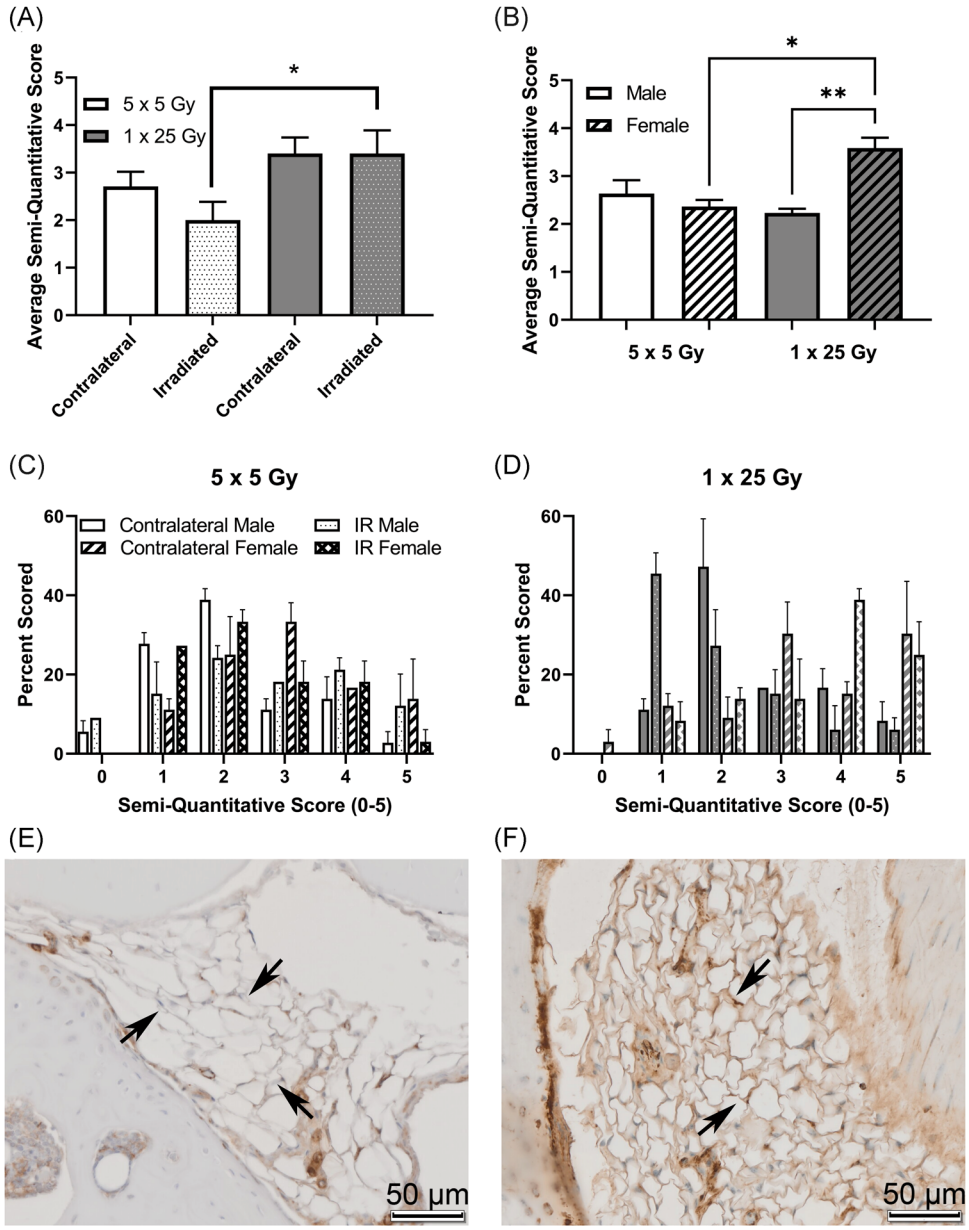

FIGURE 5 α-SMA is higher in the single-dose radiation group, and that difference is driven by female mice. Mice were scored based on a semi-quantitative guide of 0–5 (examples, Figure S4), and the average score of all mice (A), male and female mice (B), or the histogram of the percent of times that a group was scored in the 5 × 5 group (C) or the 1 × 25 group (D). Representative images are shown of negative staining (E) and positive staining (F). Images are taken of the infrapatellar fat pad, or Hoffa's fat pad, roughly midway through the joint, with the bone surrounding the fat tissue, where the staining was noticeably concentrated. Arrows indicate fat tissue where either an obvious lack of staining (E) or strong staining (F) is present. (A) 5 × 5 ($n = 6$); 1 × 25 ($n = 6$); (B) Male ($n = 3$); Female ($n = 3$); *$p < 0.03$; **$p < 0.002$, Friedman test

contracture from 20 to 30 Gy, and at doses above that, deeper tissue was responsible. Later, Stone demonstrated that fractionated doses spared some of the normal tissue damage and that overall contracture over a long timeframe is due to multiple problems including skin contracture, subcutaneous fibrosis, muscle damage, and slowed bone growth.[24] We built upon this to show that a single dose of 25 Gy is sufficient to demonstrate joint contracture that is not due to skin fibrosis. We have also shown differences in fibrosis-associated markers and contracture of deeper tissues with fractionation, supporting the preclinical utility of this model. Notably, when the skin was removed from apparent cases of arthrofibrosis, it was clear that the entire stifle and all compositional tissues had become a milieu of collagenous bands and scars that were infiltrating and connecting muscle, fat, and joint space alike.

As noted in the introduction, we did not observe any effects of the SOD mimetic treatments, disproving our initial hypothesis. However, we were also unable to confirm delivery to the specific

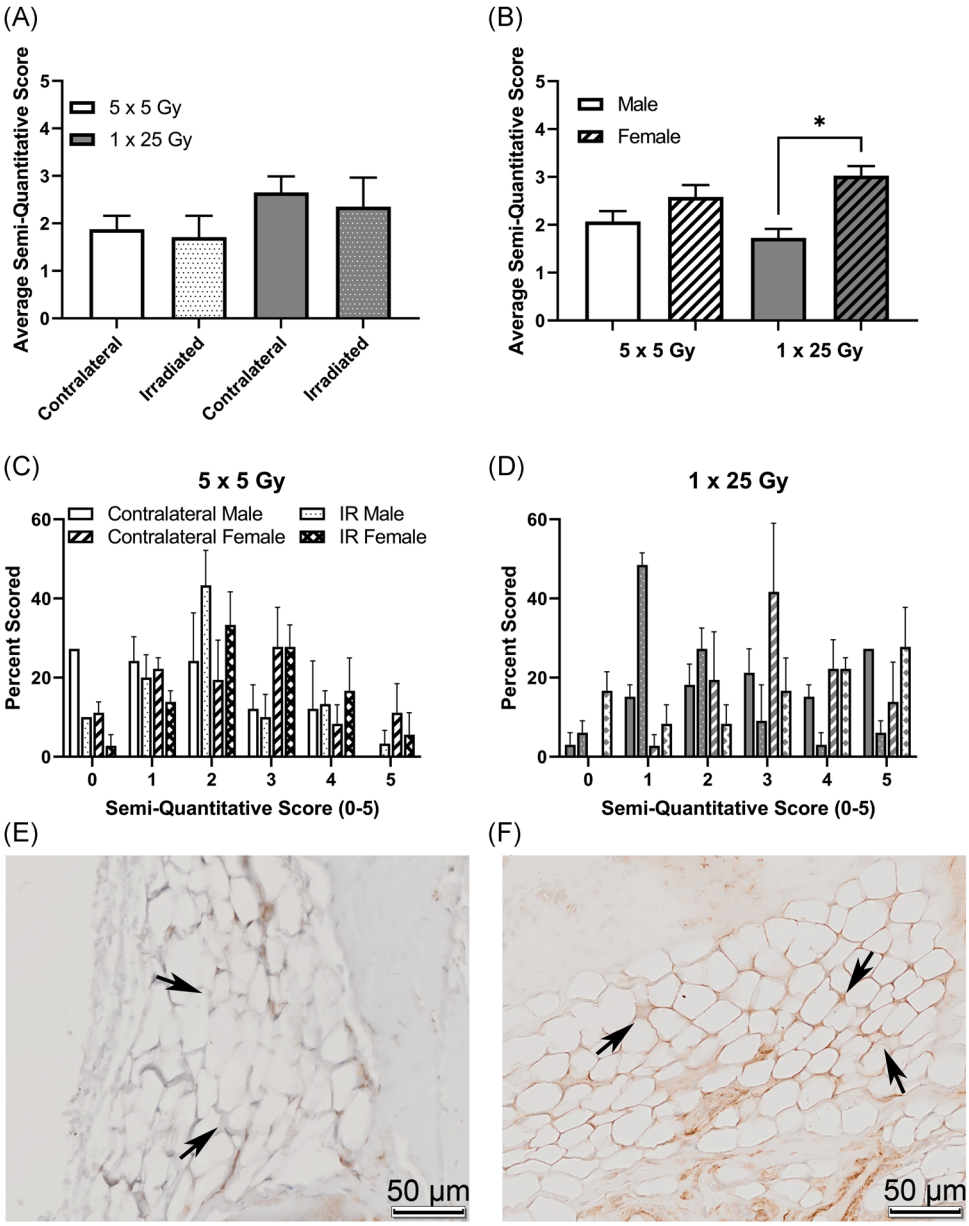

FIGURE 6 NOX4 is higher in the single dose radiation group, and that difference is driven by female mice. Mice were scored based on a semi-quantitative guide of 0–5, and the average score of all mice (A), male and female mice (B), or the histogram of the percent of times that a group was scored in the 5 × 5 group (C) or the 1 × 25 group (D). Representative images are shown of negative staining (E) and positive staining (F). Images are taken from the infrapatellar fat pad, or Hoffa's fat pad, roughly midway through the joint, with bone surrounding the fat tissue, where the staining was noticeably concentrated. Arrows indicate fat tissue where either obvious lack of staining (E) or strong staining (F) is present. (A) 5 × 5 ($n = 6$); 1 × 25 ($n = 6$); (B) Male ($n = 3$); Female ($n = 3$); *$p < 0.02$, Friedman test

tissues of the intact joint. Future applications of these compounds may be more effective for orthopedic settings when applied locally, potentially subcutaneously or proximal to the joint in another compartment. Independent of the effects of the mimetics, the strength of the sex-based differences observed was surprising. Our findings indicated that female mice develop more injuries more quickly and had more severe fibrosis and more positive staining for all of fibrosis markers compared to the males. This could be due to hormonal effects, the difference in fat deposition between males and females, or other compositional differences. It has been shown in other tissues that females show a higher long-term sensitivity to ionizing radiation than males.[15] We will continue to explore these sex-based effects of radiation-induced fibrosis in vivo and in vitro to determine the cause of the differences we observed.

We have made several qualitative observations of the stifle joint in both irradiated and contralateral legs and observed a trend toward increased capsular thickening in the irradiated legs. The intensity of both the myofibroblast marker α-SMA and the redox enzyme NOX4 were increased in the single-dose compared

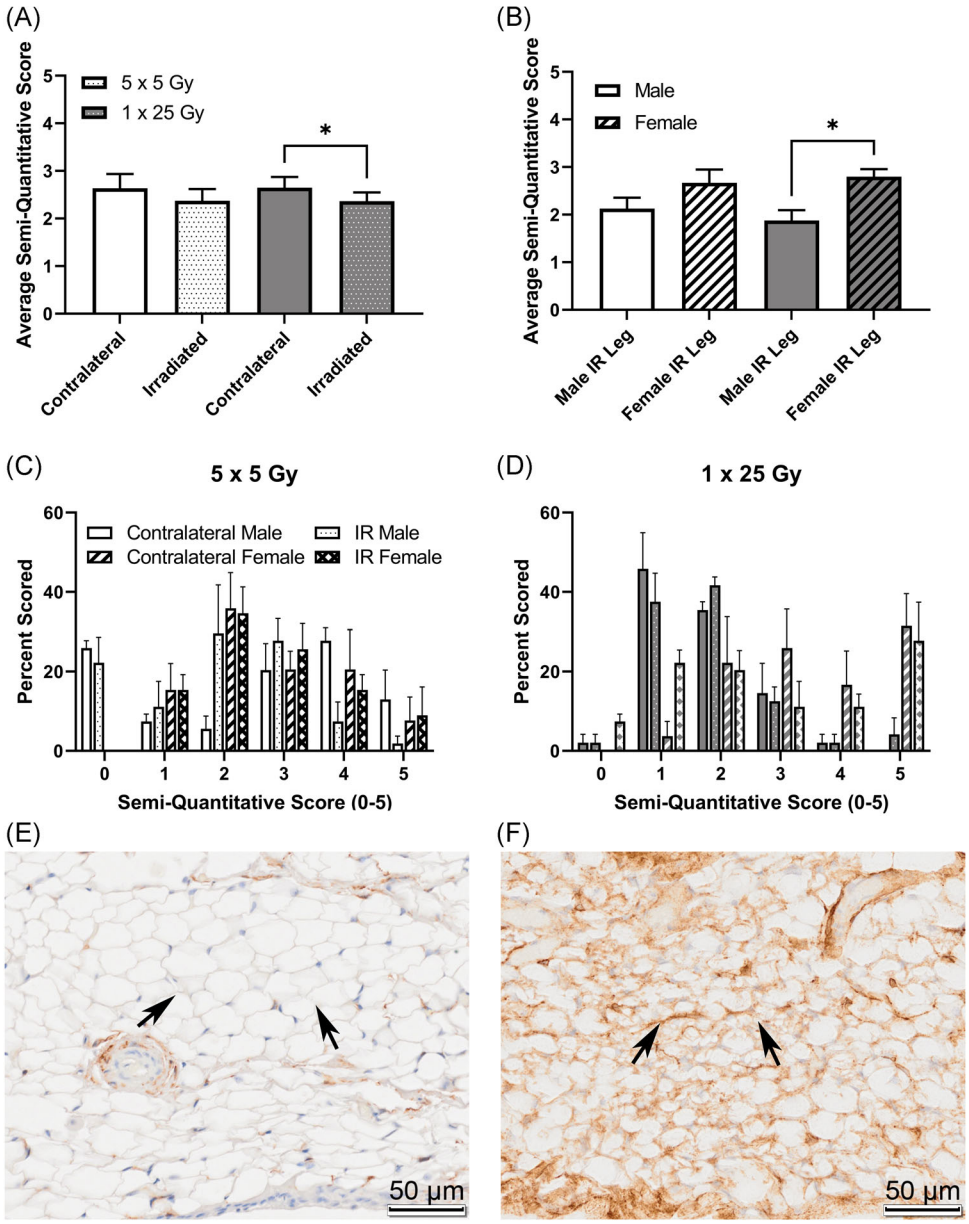

FIGURE 7 CD34 is higher in the unirradiated leg compared to the irradiated leg, and that difference is driven by female mice. Mice were scored based on a semi-quantitative guide of 0–5, and the average score of all mice (A), male and female mice (B), or the histogram of the percent of times that a group was scored in the 5 × 5 group (C) or the 1 × 25 group (D). Representative images are shown of negative staining (E) and positive staining (F). Images are taken from the infrapatellar fat pad, or Hoffa's fat pad, roughly midway through the joint, where the staining was noticeably concentrated. Arrows indicate fat tissue where either an obvious lack of staining (E) or strong staining (F) is present. (A) 5 × 5 ($n = 6$); 1 × 25 ($n = 6$); (B) Male ($n = 3$); Female ($n = 3$); *$p < 0.025$, Friedman test

with the fractionated dose. This supports that α-SMA is a positive marker for arthrofibrosis in this disease model and also implicates NOX4 in the development of joint contracture. Adipose tissue was heavily stained for markers for fibrosis and strong αSMA staining indicates that cells in the adipose tissue are expressing the myofibroblast marker when exposed to radiation. Furthermore, the marker for preadipocyte stem-ness, CD34, showed a decrease in staining in the adipose tissue of irradiated legs compared with unirradiated legs. These disruptions in adipocyte progenitor populations agree with previous literature in other tissues and may indicate a source of myofibroblasts driving disease development.[16,25,26] The potential of preadipocytes to contribute to the myofibroblast population would also help explain the difference between stifle (which has higher fat content showed signs of significant contracture and fibrosis), and hock (which remained flexible and mobile). Functional differences between these two joints are also likely to play a role in disease formation.

A variety of specific limitations of this study are worth noting. Despite both the stifle and hock joints being exposed to the

radiation field, only the stifle joint developed contracture. This might support the hypothesis that a difference in tissue composition, such as fat deposition, could be playing a critical role in the development of joint contracture. However, this preliminary study is limited to comparing these two different joints on the same animal and cannot discern the effects of adiposity compared to the specific functional and mechanical differences between the joints. Nonetheless, it is noteworthy that a fairly large percentage of stifle joints fibrosed without any indication of disease in the hock. Future studies will modulate fat content and adipocyte differentiation around the same joint to interrogate the involvement of fat more directly. Alternatively, our results may indicate that functional differences between the stifle and hock are important to preventing arthrofibrosis. This may be important for developing physical therapy routines for patients.

Another limitation of our study is that our fractionated doses were only given for 5 days, and in the future preclinical investigations of therapeutic approaches would need to be given for a longer period to mimic conventional radiotherapy. To that end, mice were killed after 12 weeks to correspond to the earliest reports of noticeable arthrofibrosis from Stone[23] with the intention of this likely corresponding to the earliest time when patients might notice problems with their joint function and seek clinical care. The relatively low prevalence of joint contracture in conjunction with our overall injury data suggests to us that joint contracture is dependent upon ongoing injury responses related to the initial radiation-induced injury, that is, mice that demonstrated observable injuries from radiation were those mice who later demonstrated joint contracture. It should be noted that despite staying far below the dose constraints in human bone and joint spaces, we still saw a physiological and biological difference after only 12 weeks. Mice used in this study were relatively young compared to the comparative age of human cancer patients; thus, it may be valuable to determine whether young and old mice have a differential response to this radiation injury in the future. More importantly, this relatively young age may be crucial to the sex-based differences observed and future studies may concentrate on risks to younger patients' joints. Finally, an important limitation in this study was the use of C57B6J mice, and future studies will incorporate the normal B6 strain for comparison between labs.

Overall, we have shown that adipose tissue is directly involved in arthrofibrosis resulting from IR exposure like radiotherapy. We also have demonstrated a clear sex-dependent response in the severity of the disease. Moving forward we intend to further examine the mechanisms behind the differential response between the male and female mice. These sex-dependent responses are critical to providing future patient care and ensuring that patients are best prepared for the long-term effect of radiation therapy.

ACKNOWLEDGEMENTS

This study was funded by the NIH (5R00AR070914-03) and (5T32CA078586-20).

CONFLICT OF INTERESTS

The authors declare no conflict of interests.

AUTHOR CONTRIBUTIONS

Substantial contributions to research design, or the acquisition, analysis, or interpretation of data: S. Rodman, P. Kluz, M. Hines, and M. Coleman. Drafting the paper or revising it critically: S. Rodman, P. Kluz, M. Hines, R. Oberley-Deegan, and M. Coleman. Approval of the submitted and final versions: S. Rodman and M. Coleman. All authors reviewed the results and approved the final version of the manuscript.

ORCID

Mitchell C. Coleman http://orcid.org/0000-0002-5116-801X

REFERENCES

1. Siegel RL, Miller KD, Fuchs HE, Jemal A. Cancer Statistics, 2021. *CA Cancer J Clin*. 2021;71:7-33.
2. Delaney G, Jacob S, Featherstone C, Barton M. The role of radiotherapy in cancer treatment: estimating optimal utilization from a review of evidence-based clinical guidelines. *Cancer*. 2005;104:1129-1137.
3. Saintigny Y, Cruet-Hennequart S, Hamdi DH, Chevalier F, Lefaix JL. Impact of therapeutic irradiation on healthy articular cartilage. *Radiat Res*. 2015;183:135-146.
4. Bryant AK, Banegas MP, Martinez ME, Mell LK, Murphy JD. Trends in radiation therapy among cancer survivors in the United States, 2000-2030. *Cancer Epidemiol Biomarkers Prev*. 2017;26:963-970.
5. Bluethmann SM, Mariotto AB, Rowland JH. Anticipating the "Silver Tsunami": prevalence trajectories and comorbidity burden among older cancer survivors in the United States. *Cancer Epidemiol Biomarkers Prev*. 2016;25:1029-1036.
6. Johansson S, Svensson H, Denekamp J. Dose response and latency for radiation-induced fibrosis, edema, and neuropathy in breast cancer patients. *Int J Radiat Oncol Biol Phys*. 2002;52:1207-1219.
7. Moloney EC, Brunner M, Alexander AJ, Clark J. Quantifying fibrosis in head and neck cancer treatment: an overview. *Head Neck*. 2015;37:1225-1231.
8. Stinson SF, DeLaney TF, Greenberg J, et al. Acute and long-term effects on limb function of combined modality limb sparing therapy for extremity soft tissue sarcoma. *Int J Radiat Oncol Biol Phys*. 1991;21:1493-1499.
9. Straub JM, New J, Hamilton CD, Lominska C, Shnayder Y, Thomas SM. Radiation-induced fibrosis: mechanisms and implications for therapy. *J Cancer Res Clin Oncol*. 2015;141:1985-1994.
10. Wong K, Trudel G, Laneuville O. Noninflammatory joint contractures arising from immobility: animal models to future treatments. *BioMed Res Int*. 2015;2015:848290.
11. Nwachukwu BU, McFeely ED, Nasreddine A, et al. Arthrofibrosis after anterior cruciate ligament reconstruction in children and adolescents. *J Pediatr Orthop*. 2011;31:811-817.
12. Sanders TL, Kremers HM, Bryan AJ, Kremers WK, Stuart MJ, Krych AJ. Procedural intervention for arthrofibrosis after ACL reconstruction: trends over two decades. *Knee Surg Sports Traumatol Arthrosc*. 2017;25:532-537.
13. Usher KM, Zhu S, Mavropalias G, Carrino JA, Zhao J, Xu J. Pathological mechanisms and therapeutic outlooks for arthrofibrosis. *Bone Res*. 2019;7:9.
14. Klein SL, Flanagan KL. Sex differences in immune responses. *Nat Rev Immunol*. 2016;16:626-638.

15. Narendran N, Luzhna L, Kovalchuk O. Sex difference of radiation response in occupational and accidental exposure. *Front Genet*. 2019;10:260.
16. Bourlier V, Sengenès C, Zakaroff-Girard A, et al. TGFbeta family members are key mediators in the induction of myofibroblast phenotype of human adipose tissue progenitor cells by macrophages. *PLoS One*. 2012;7:e31274.
17. Jeong W, Yang X, Lee J, et al. Serial changes in the proliferation and differentiation of adipose-derived stem cells after ionizing radiation. *Stem Cell Res Ther*. 2016;7:117.
18. Mapuskar KA, Anderson CM, Spitz DR, Batinic-Haberle I, Allen BG, E Oberley-Deegan R. Utilizing superoxide dismutase mimetics to enhance radiation therapy response while protecting normal tissues. *Semin Radiat Oncol*. 2019;29:72-80.
19. Batinic-Haberle I, Tovmasyan A, Spasojevic I. Mn porphyrin-based redox-active drugs: differential effects as cancer therapeutics and protectors of normal tissue against oxidative injury. *Antioxid Redox Signal*. 2018;29:1691-1724.
20. Chatterjee A, Zhu Y, Tong Q, Kosmacek E, Lichter E, Oberley-Deegan R. The addition of manganese porphyrins during radiation inhibits prostate cancer growth and simultaneously protects normal prostate tissue from radiation damage. *Antioxidants (Basel)*. 2018;7:7.
21. Mapuskar KA, Wen H, Holanda DG, et al. Persistent increase in mitochondrial superoxide mediates cisplatin-induced chronic kidney disease. *Redox Biol*. 2019;20:98-106.
22. Emami B, Lyman J, Brown A, et al. Tolerance of normal tissue to therapeutic irradiation. *Int J Radiat Oncol Biol Phys*. 1991;21:109-122.
23. Stone HB. Leg contracture in mice: an assay of normal tissue response. *Int J Radiat Oncol Biol Phys*. 1984;10:1053-1061.
24. Masuda K, Hunter N, Stone HB, Withers HR. Leg contracture in mice after single and multifractionated 137Cs exposure. *Int J Radiat Oncol Biol Phys*. 1987;13:1209-1215.
25. Díaz-Flores L, Gutiérrez R, García MP, et al. CD34+ stromal cells/fibroblasts/fibrocytes/telocytes as a tissue reserve and a principal source of mesenchymal cells. Location, morphology, function and role in pathology. *Histol Histopathol*. 2014;29:831-870.
26. Onuora S. Connective tissue diseases: adipocyte-myofibroblast transition: linking intradermal fat loss to skin fibrosis in SSc. *Nat Rev Rheumatol*. 2015;11:63.

SUPPORTING INFORMATION

Additional supporting information may be found in the online version of the article at the publisher's website.

How to cite this article: Rodman SN, Kluz PN, Hines MR, Oberley-Deegan RE, Coleman MC. Sex-based differences in the severity of radiation-induced arthrofibrosis. *J Orthop Res*. 2022;40:2586-2596. doi:10.1002/jor.25297